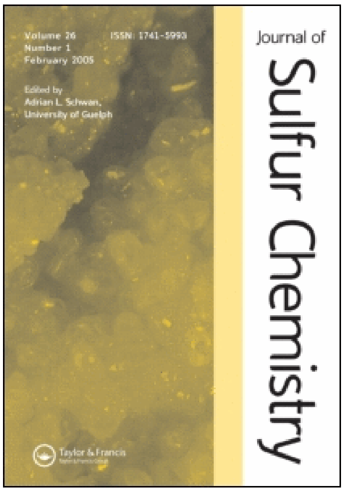

Journal of Sulfur Chemistry
Publication details, including instructions for authors and subscription information:
http://www.informaworld.com/smpp/title~content=t713926081

SNO donor Schiff bases and their Co(II), Ni(II) and Cu(II) complexes: synthesis, characterization, electrochemical and antimicrobial studies

Ajaykumar D. Kulkarni[a]; Sangamesh A. Patil[a]; Prema S. Badami[b]
[a] PG Department of Chemistry, Karnatak University, Dharwad, Karnataka, India [b] Department of Chemistry, Shri Sharanabasaveswar College of Science, Gulbarga, Karnataka, India

To cite this Article Kulkarni, Ajaykumar D. , Patil, Sangamesh A. and Badami, Prema S.(2009) 'SNO donor Schiff bases and their Co(II), Ni(II) and Cu(II) complexes: synthesis, characterization, electrochemical and antimicrobial studies', Journal of Sulfur Chemistry, 30: 2, 145 — 159

To link to this Article: DOI: 10.1080/17415990802663133

URL: http://dx.doi.org/10.1080/17415990802663133

Journal of Sulfur Chemistry
Vol. 30, No. 2, April 2009, 145–159

Taylor & Francis
Taylor & Francis Group

SNO donor Schiff bases and their Co(II), Ni(II) and Cu(II) complexes: synthesis, characterization, electrochemical and antimicrobial studies

Ajaykumar D. Kulkarni[a], Sangamesh A. Patil[a]*, and Prema S. Badami[b]

[a] PG Department of Chemistry, Karnatak University, Dharwad, Karnataka, India; [b] Department of Chemistry, Shri Sharanabasaveswar College of Science, Gulbarga, Karnataka, India

(*Received 20 October 2008; final version received 3 December 2008*)

A series of Co(II), Ni(II) and Cu(II) complexes have been synthesized with newly synthesized Schiff bases derived from 3-substituted-4-amino-5-mercapto-1,2,4-triazole and isatin. The elemental analyses of the complexes are confined to the stoichiometry of the type ML_2 [M=Co(II), Ni(II) and Cu(II)], respectively, where L acts as a deprotonated ligand in which sulfur plays an important role in coordination. In view of analytical, spectroscopic, magnetic and thermal studies, it has been concluded that the Co(II), Ni(II) and Cu(II) complexes possess octahedral geometry. The redox behavior of the complexes investigated with the aid of cyclic voltammetry indicated the two-electron transfer process. The antimicrobial studies of Schiff bases and their complexes against various antibacterial (*Escherichia coli, Staphylococcus aureus, Pseudomonas aeruginosa* and *Bacillus subtilis*) and antifungal (*Aspergillus niger* and *Pencillium chrysogenum*) species by the minimum inhibitory concentration method revealed that the Schiff bases and some of their metal complexes possess more healing antibacterial activity.

Keywords: antimicrobial; electrochemical; isatin; NMR; spectral; triazoles

1. Introduction

The S, N and O atoms play a key role in the coordination of metals at the active sites of numerous metallobiomolecules. The chemistry of 1,2,4-triazole derivatives has attracted widespread attention due to their diverse biological activities and they are a new class of antimicrobial agents (*1, 2*) viz. fluconazole and itraconazole are used as antimicrobial drugs. Hence, the metal complexes of Schiff bases derived from 1,2,4-triazole derivatives have been the subject of considerable study (*3–8*). A number of metal complexes with 1,2,4-triazole Schiff bases have been reported from our laboratory (*9–12*). In addition to this, isatin, which is an endogenous indole, and its derivatives have also been shown to exhibit a wide range of biological activities (*13–18*). Moreover, it has been largely used as a versatile reagent in organic synthesis to obtain heterocyclic compounds, and as a raw material for drugs (*19*). Some Schiff bases derived from isatin were prepared by reaction with amino acids or substituted hydrazines and were subsequently metallated with

---

*Corresponding author. Email: patil1956@rediffmail.com

ISSN 1741-5993 print/ISSN 1741-6000 online

DOI: 10.1080/17415990802663133
http://www.informaworld.com

nickel(II), copper(II), zinc(II) or cobalt(II) ions (*20, 21*). Recently, it has been reported that the isatin-thiosemicarbazone copper(II) complexes related to the antiviral drug methisazone, were prepared electrochemically or by usual condensation methods (*22*). Since triazoles are heterocyclic compounds and Schiff bases derived from isatin often act as versatile chelating agents and exhibit promising bioactivities, it is likely that isatin–triazoles and their metal complexes might also exhibit useful biological activity.

Thus, the present study aims to synthesize a new series of Co(II), Ni(II) and Cu(II) complexes with novel Schiff base molecules derived from 3-substituted-4-amino-5-mercapto-1,2,4-triazole and isatin. Analytical, spectral, magnetic and thermal characterization techniques are employed. The electron transfer process of the metal complexes is investigated. In the light of the wide spectrum of microbial activity, the Schiff bases and their metal complexes were screened for their antibacterial and antifungal activities.

2. Experimental

2.1. *Physical measurements*

Carbon, hydrogen and nitrogen were estimated using Elemental Analyzer Carlo Erba EA1108 analyzer. The IR spectra of the Schiff bases and their Co(II), Ni(II) and Cu(II) complexes were recorded on a HITACHI-270 IR spectrophotometer in the 4000–250 cm^{-1} region in KBr disc. The electronic spectra of the complexes were recorded in HPLC grade dimethyl formamide (DMF) and DMSO on a VARIAN CARY 50-BIO UV-spectrophotometer in the region of 200–1100 nm. The ^{1}H- nuclear magnetic resonance (NMR), ^{13}C-NMR and 2D NMR spectra of the ligands were recorded in d$_6$-DMSO on a BRUKER 300 MHz spectrometer at room temperature using TMS as an internal reference. FAB-mass spectra were recorded on a JEOL SX 102/DA-6000 mass spectrometer/data system using Argon/Xenon (6 kV, 10 A) as the FAB gas. The accelerating voltage was 10 kV, and the spectra were recorded at room temperature and m-nitrobenzyl alcohol was used as the matrix. The mass spectrometer was operated in the positive ion mode. The ESR spectrum was recorded on a Varian-E-4X-band EPR spectrometer and the field set is 3000 G at modulation frequency of 100 K Hz under liquid nitrogen temperature using TCNE as g marker. Thermogravimetric analyses data were measured from room temperature to 1000 °C at a heating rate of 10 °C min^{-1}. The data were obtained using a PERKIN-ELMER DIAMOND TG/DTA instrument. Electrochemical behavior of the Co(II), Ni(II) and Cu(II) complexes were studied on a CHI1110A-Electrochemical analyzer (made in the USA) in HPLC grade DMF containing 0.05 M n-Bu$_4$NClO$_4$ as the supporting electrolyte. The three-electrode system consisted of glassy carbon (working), platinum wire (counter) and Ag/AgCl (reference) electrodes. Molar conductivity measurements were recorded on ELICO-CM-82 T Conductivity Bridge with a cell having cell constant 0.51, and magnetic moment was carried out using Faraday balance.

2.2. *Materials*

All the chemicals used were of reagent grade. 3-substituted-4-amino-5-mercapto-1,2,4-triazole was synthesized according to the literature (*23, 24*). Isatin was recrystallized before using.

2.2.1. *Synthesis of Schiff bases (**I–IV**)*

The synthesis of Schiff bases is schematically presented in Scheme 1. The Schiff bases have been synthesized by refluxing the reaction mixture of hot methanolic solution (30 mL) of

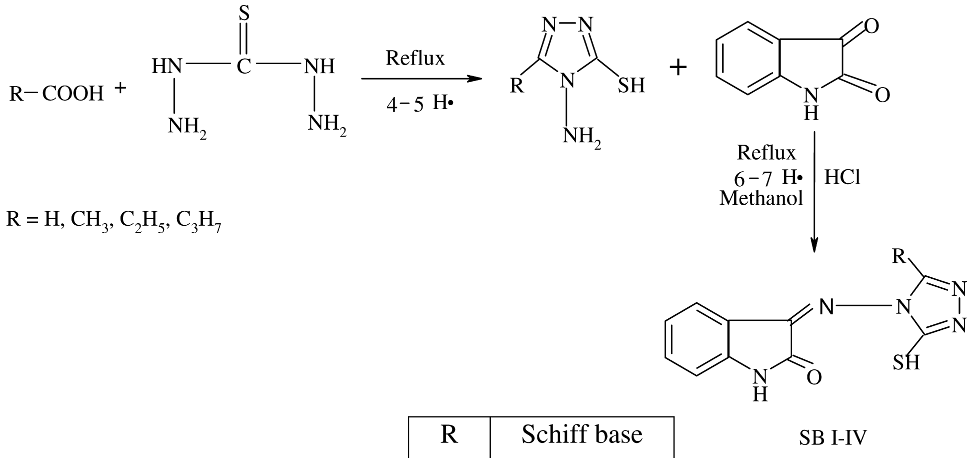

R	Schiff base no.
H	**SB I**
CH_3	**SB II**
C_2H_5	**SB III**
C_3H_7	**SB IV**

Scheme 1. Synthesis of Schiff bases I–IV.

3-substituted-4-amino-5-mercapto-1,2,4-triazole (0.01 mol) and hot methanolic solution (30 mL) of isatin (0.01 mol) for 6–7 h with a few drops of hydrochloric acid. The product obtained after the evaporation of the solvent was filtered, washed with cold MeOH and recrystallized from MeOH. Yield (M.P.): 78% (188 °C), 76 % (192 °C), 81% (195 °C) and 79% (196 °C) of **SB-I, SB-II, SB-III** and **SB-IV**, respectively.

2.2.2. *Synthesis of Co(II), Ni(II) and Cu(II) complexes (*1–12*)*

Methanolic solution (45 mL) of Schiff base (1 mmol) was mixed with methanolic solution (5 mL) of $CoCl_2.6H_2O$/$NiCl_2.6H_2O$/$CuCl_2.2H_2O$ (1 mmol) and refluxed on water bath for 2 h. Then, to the reaction mixture 2 mmol of sodium acetate was added and refluxion was continued for 2 h. The separated complex was filtered, washed thoroughly with water and methanol and dried in vacuum over fused $CaCl_2$. Yield of all the metal complexes lie in the range of 67–73%.

2.3. **In vitro** ***antibacterial and antifungal assay***

The biological activities of synthesized Schiff bases and their Co(II), Ni(II) and Cu(II) complexes were studied for their antibacterial and antifungal activities by agar and potato dextrose agar diffusion method, respectively. The antibacterial and antifungal activities were done at 100, 200 and 500 $\mu g\ mL^{-1}$ concentrations in DMF solvent using four bacteria (*Escherichia coli, Staphylococcus aureus, Pseudomonas aeruginosa* and *Bacillus subtilis)* and two fungi (*Aspergillus niger* and *Pencillium chrysogenum)* strains by the minimum inhibitory concentration (MIC) method (25). These bacterial and fungi strains were incubated for 24 h at 37 °C and for 48 h at 37 °C, respectively. Standard antibacterial (*Streptomycin*) and antifungal drugs (*Nyastatin*) were used for comparison under similar conditions. Activity was determined by measuring the diameter of the zone showing complete inhibition (mm).

3. Results and discussion

The Schiff bases (**I–IV**) form octahedral complexes (**1–12**) (Table 1) with $CoCl_2.6H_2O/NiCl_2.6H_2O/CuCl_2.2H_2O$ in methanol. All the Co(II), Ni(II) and Cu(II) complexes are stable and non-hygroscopic in nature. The complexes are insoluble in common organic solvents but soluble in DMF and DMSO. The elemental analyses show that the Co(II), Ni(II) and Cu(II) complexes have 1:2 stoichiometry of the type ML_2, where L stands for a deprotonated ligand and exhibit thiol–thione tautomerism (Figure 1). The molar conductance values are too low to account for any dissociation of the complexes in DMF, indicating the non-electrolytic nature of the complexes in DMF (Table 1). Several attempts made to develop the single crystal of the complexes failed due to insolubility of the complexes in common organic solvents.

3.1. *IR spectral studies*

The prominent infrared spectral data of Schiff bases and their Co(II), Ni(II) and Cu(II) complexes are presented in Tables 2 and 3, respectively.

The IR spectra of the Schiff bases exhibited characteristic bands due to ν(NH) of isatin in the region 3110–3198 cm^{-1}. A characteristic strong band at 2693–2702 cm^{-1} is ascribed to ν(SH) of triazole and another band around ~1100 cm^{-1} is assigned to ν(C=S) (*26*). These observations suggest that the Schiff bases exhibit thiol–thione tautomerism (Figure 1). In addition, the strong band at 1730–1738 cm^{-1} and a characteristic high intensity band at 1614–1617 cm^{-1} in the IR spectra of the Schiff bases are assigned to lactonyl carbon ν(C=O) and ν(C=N), respectively (*27*).

In comparison with the spectra of the Schiff bases, all the Co(II), Ni(II) and Cu(II) complexes exhibited the band of ν(C=N) in the region 1590–1603 cm^{-1}, showing the shift of the band to lower wave numbers and indicating that the nitrogen is coordinated to the metal ion (*21, 28, 29*). The band of ν(C=O) in the region 1708–1722 cm^{-1} in the complexes, showing the shift to lower wave numbers compared with Schiff bases confirms that the carbonyl oxygen, is coordinated to the metal ion (*30, 31*).

The deprotonation of the thiol group is indicated by the absence of a band around ~ 2700 cm^{-1} in all the metal complexes, which is due to ν(S−H) of Schiff bases, indicating that the metal is coordinated through the sulfur atom. This is further supported by the band around ~ 750 cm^{-1} in the metal complexes due to ν(C−S). The unaltered position of a band due to ν(NH) in all the metal complexes indicates that the nitrogen atom of isatin is not involved in coordination.

The new bands in the region of 452–480 cm^{-1} in the spectra of the complexes are assigned to stretching frequencies of (M–N) bonds. The band in the region 333–379 cm^{-1} of far IR-spectra is due to metal-sulfur bond formation.

Thus, the IR spectral data results provide strong evidence for the complexation of Schiff bases with metal (II) ions.

3.2. *NMR studies of Schiff bases*

The Schiff bases have been characterized by ^1H and ^{13}C NMR spectra and also $2D^1H$-^{13}C HETCOR to ensure ligand purity in solution, and elucidate the differently positioned proton and carbon.

The proton NMR of Schiff base **III** is discussed here and the data of ^1H NMR of all the Schiff bases is presented in Table 4. In the ^1H NMR spectrum of the Schiff base (III), the NH proton of isatin exhibited signals at 11.9 ppm (s, 1H), and the signal observed at 11 ppm (s, 1H)

Table 1. Elemental analyses of Schiff bases and their Co(II), Ni(II) and Cu(II) complexes along with molar conductance and magnetic moment data.

Compound number	Empirical formula	M%		C%		H%		N%		Molar conductance, $\text{Ohm}^{-1}\,\text{cm}^2\,\text{mole}^{-1}$	μ_{eff} (BM)
		Obsd.	Calcd.	Obsd.	Calcd.	Obsd.	Calcd.	Obsd.	Calcd.		
SB I	$C_{10}H_7N_5OS$	–	–	48.97	48.98	2.85	2.86	28.57	28.57	–	–
SB II	$C_{11}H_9N_5OS$	–	–	50.96	50.96	3.48	3.47	27.02	27.03	–	–
SB III	$C_{12}H_{11}N_5OS$	–	–	52.74	52.75	4.03	4.02	25.65	25.64	–	–
SB IV	$C_{13}H_{13}N_5OS$	–	–	54.35	54.36	4.52	4.52	24.39	24.39	–	–
1	$Co(C_{10}H_6N_5OS)_2$	10.46	10.55	42.86	42.93	2.10	2.14	25.13	25.04	17	4.61
2	$Co(C_{11}H_8N_5OS)_2$	10.24	10.26	45.90	45.91	2.88	2.78	24.23	24.34	21	4.72
3	$Co(C_{12}H_{10}N_5OS)_2$	9.71	9.78	47.61	47.76	3.26	3.31	23.23	23.22	19	4.86
4	$Co(C_{13}H_{12}N_5OS)_2$	9.26	9.35	49.44	49.44	3.71	3.88	22.26	22.18	23	4.74
5	$Ni(C_{10}H_6N_5OS)_2$	10.32	10.39	42.91	43.01	2.20	2.15	25.11	25.08	18	3.10
6	$Ni(C_{11}H_8N_5OS)_2$	10.03	10.10	45.80	45.99	2.78	2.79	24.28	24.39	24	3.08
7	$Ni(C_{12}H_{10}N_5OS)_2$	9.56	9.63	47.81	47.84	3.21	3.32	23.26	23.25	17	3.24
8	$Ni(C_{13}H_{12}N_5OS)_2$	9.28	9.20	49.49	49.52	3.70	3.80	22.17	22.22	22	3.18
9	$Cu(C_{10}H_6N_5OS)_2$	11.24	11.19	42.60	42.62	2.20	2.13	24.90	24.86	16	1.75
10	$Cu(C_{11}H_8N_5OS)_2$	10.76	10.88	45.43	45.59	2.74	2.76	24.18	24.17	25	1.77
11	$Cu(C_{12}H_{10}N_5OS)_2$	10.36	10.37	47.39	47.44	3.15	3.29	23.17	23.06	20	1.75
12	$Cu(C_{13}H_{12}N_5OS)_2$	9.96	9.92	49.10	49.13	3.98	3.78	22.10	22.04	21	1.74

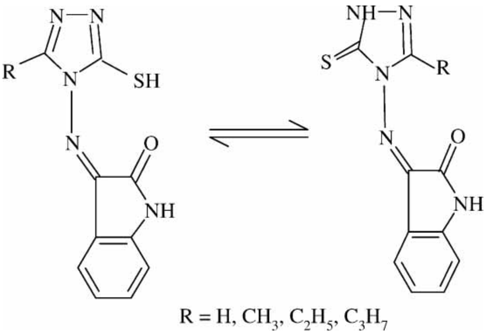

Figure 1. Structure of Schiff bases I–IV : thiol–thione tautomerism.

Table 2. The important infrared frequencies (in cm^{-1}) of Schiff bases derived from 3-substituted-4-amino-5-mercapto-1,2,4-triazole and isatin.

Compound number	Lactonyl, ν(C=O) of indole ring	ν(C=N)	ν (NH) of indole ring	ν (SH)	ν(C=S)
$C_{10}H_7N_5OS$	1732	1615	3198	2702	1102
$C_{11}H_9N_5OS$	1730	1616	3185	2701	1098
$C_{12}H_{11}N_5OS$	1738	1614	3110	2693	1100
$C_{13}H_{13}N_5OS$	1730	1617	3192	2698	1095

Table 3. The important infrared frequencies (in cm^{-1}) of metal complexes.

Compound number	Indole ring, ν (NH)	Lactonyl, ν (C=O)	ν (C=N)	ν (C-S)	ν (M-N)	ν (M-S)
$Co(C_{10}H_6N_5OS)_2$	3202	1721	1603	750	461	361
$Co(C_{11}H_8N_5OS)_2$	3187	1716	1590	752	455	354
$Co(C_{12}H_{10}N_5OS)_2$	3115	1722	1596	758	476	333
$Co(C_{13}H_{12}N_5OS)_2$	3194	1711	1592	753	480	379
$Ni(C_{10}H_6N_5OS)_2$	3196	1718	1602	752	464	365
$Ni(C_{11}H_8N_5OS)_2$	3181	1714	1592	754	452	358
$Ni(C_{12}H_{10}N_5OS)_2$	3114	1715	1590	759	478	341
$Ni(C_{13}H_{12}N_5OS)_2$	3194	1713	1601	752	471	376
$Cu(C_{10}H_6N_5OS)_2$	3198	1715	1598	751	463	363
$Cu(C_{11}H_8N_5OS)_2$	3183	1711	1596	752	458	351
$Cu(C_{12}H_{10}N_5OS)_2$	3114	1722	1591	756	471	338
$Cu(C_{13}H_{12}N_5OS)_2$	3196	1708	1602	754	478	378

Table 4. The important ^1H NMR and ^{13}C NMR data of Schiff bases.

Schiff base number	^1H NMR (d_6 DMSO) (ppm)	^{13}C NMR (d_6 DMSO) (ppm)
$C_{10}H_7N_5OS$	11.6 (s, 1H, NH), 10.1 (s, 1H, SH), 6.1–7.1 (m, 4H, Ar-H), 6.9 (s, 1H, CH of triazole)	113.1, 118.6, 125.5, 126.7, 144.6, 155.2, (isatin), 139.1 (C=N), 160 (C=O), 185, 172 (triazole)
$C_{11}H_9N_5OS$	11.7 (s, 1H, NH), 10.4 (s, 1H, SH), 6.3–7.2 (m, 4H, Ar-H), 2.7 (s, 3H, CH_3)	113.1, 118.6, 125.5, 126.7, 144.6, 155.2, (isatin), 139.5 (C=N), 162 (C=O), 185, 176 (triazole), 34.4(CH_3)
$C_{12}H_{11}N_5OS$	11.9 (s, 1H, NH), 11.0 (s, 1H, SH), 6.9–7.5 (m, 4H, Ar-H), 2.2(q, 2H, CH_2), 1.3(t, 3H, CH_3)	113.1, 118.6, 125.5, 126.7, 144.6, 155.2, (isatin), 139.3 (C=N), 165 (C=O), 185, 178 (triazole), 11.1 (CH_3), 31.5 (CH_2)
$C_{13}H_{13}N_5OS$	12.1 (s, 1H, NH), 11.03 (s, 1H, SH), 6.8–7.6 (m, 4H, Ar-H), 2.4 (t, 2H, CH_2), 2.2 (m, 2H, CH_2), 1.2 (t, 3H, CH_3)	113.1, 118.6, 125.5, 126.7, 144.6, 155.2, (isatin), 139.3 (C=N), 160 (C=O), 185, 182 (triazole), 11.1 (CH_3), 18.8 (CH_2), 31.5(CH_2)

is due to S–H proton. The multiplet signals around 6.9–7.5 ppm (m, 4H) are ascribed to aromatic protons. The quartet and triplet observed at 2.2 and 1.3 ppm are due to CH_2 and CH_3, respectively.

The representative ^{13}C NMR spectrum of the Schiff base **III** is discussed here. In the representative ^{13}C NMR spectrum of the Schiff base **III** the signal observed at 165 ppm is ascribed to the lactonyl carbon (C=O) of the isatin. A characteristic signal at 139.3 ppm is assigned to (C=N). In addition to this, the characteristic signals in the 113.1–155.2 ppm region are assigned to aromatic carbon, and the signals at 11.1 and 31.5 ppm are due to the CH_3 and CH_2 group attached to heterocyclic ring, respectively. The ^{13}C NMR data of all the Schiff bases is given in Table 4.

In the two dimensional HETCOR NMR spectra, the signals observed are due to the interaction of proton and carbon in which the proton values are recorded along the y-axis and carbon values are recorded along the x-axis. The representative 2D spectrum of the Schiff base **IV** is discussed here. The interaction of protons and carbons of the aromatic region are well observed in the spectrum as signals. Also, the resonance due to the interaction of protons and carbons of CH_3, CH_2 and CH_2 groups attached to the heterocyclic ring are observed as signals at corresponding coinciding points of the y and x-axis, respectively.

3.3. *Electronic spectra*

The electronic spectra of Co(II) complexes exhibited absorption bands in the regions 8000–10,000 cm^{-1} and 18,000–20,000 cm^{-1} corresponding to ν_1 and ν_3 transitions, respectively, which are attributed to the transitions $^4T_{1g}$ (F)→$^4T_{2g}$ (F) (ν_1); ^4T_1g (F)→^4T_1g (P) (ν_3). In the present investigation, brownish Co(II) complexes show the absorption bands at 8954–8968 and 19,165–19,182 cm^{-1} are corresponding to ν_1 and ν_3 transitions, respectively. These bands are the characteristic of high spin octahedral Co(II) complex (*32*). However, ν_2 band is not observed because of its proximity to strong ν_3 transition.

The greenish $Ni(C_{12}H_{10}N_5OS)_2$ complex exhibited three bands at 10,375, 15,845 and 26,345 cm^{-1} and attributed to the $^3A_{2g} \rightarrow {}^3T_{2g}$ (ν_1); $^3A_{2g} \rightarrow {}^3T_{1g}$ (F) (ν_2) and $^3A_{2g} \rightarrow {}^3T_{1g}$ (P) (ν_3) transitions, respectively, which indicate an octahedral geometry around Ni(II) ion (*33*). The ligand field parameters are given in Table 5. The value of ν_2/ν_1 is found to be around 1.527, and the μ_{eff} value is around 3.174, which is within the range of 2.8–3.5 BM, suggesting the octahedral environment. The values of the nephelauxetic parameter, β, indicate the low covalent character of the metal-ligand σ bonds (*34*). Hence the ligand field parameters correlate the electronic spectral and magnetic properties.

The electronic spectra of Cu(II) complexes display two prominent bands. A low-intensity broad band of around 14,486 cm^{-1} is assignable to $^2E_g \rightarrow {}^2T_{2g}$ transition and another high-intensity band at 25,582 cm^{-1} is due to symmetry forbidden ligand → metal charge transfer. On the basis of electronic spectra distorted octahedral geometry around Cu(II) ion is suggested (*35*).

3.4. *Magnetic studies*

The magnetic moments obtained at room temperature are listed in Table 1. The magnetic measurement for Co(II) complexes exhibit magnetic moment values of 4.61–4.86, which are in agreement with the octahedral range of 4.3–5.2 BM. Ni(II) complexes showed the magnetic moment values of 3.08–3.24 within the range of 2.8–3.5 BM, suggesting (*36*) consistency with their octahedral environment. The Cu(II) complexes showed a magnetic moment of 1.75–1.77 BM, slightly higher than the spin-only value 1.73 BM expected for one unpaired electron, which offers the possibility of an octahedral geometry (*37*).

Table 5. Ligand field parameters of Ni(II) complexes.

	Tranistions (cm^{-1})											
Complex number	ν_1	ν_2	ν_3	ν_2 Cald. cm^{-1}	Dq cm^{-1}	B^1 cm^{-1}	Distortion (%)	ν_2/ν_1	LSFE	μ_{eff}, Cald. BM	β	β (%)
$Ni(C_{10}H_6N_5OS)_2$	10,355	15,814	26,348	16,413	1035	779	3.653	1.527	35.503	3.174	0.738	26.158
$Ni(C_{11}H_8N_5OS)_2$	10,305	15,836	26,340	16,368	1030	786	3.251	1.537	35.331	3.176	0.745	25.548
$Ni(C_{12}H_{10}N_5OS)_2$	10,375	15,845	26,345	16,429	1037	776	3.558	1.527	35.571	3.174	0.735	26.455
$Ni(C_{13}H_{12}N_5OS)_2$	10,314	15,824	26,341	16,376	1031	785	3.372	1.534	35.362	3.176	0.743	25.661

3.5. *FAB-mass spectral studies*

The FAB-mass spectrum of Schiff base **III** exhibited a molecular ion peaks at m/z 273 which is equivalent to its molecular weight. The fragmentation peaks at m/z 240, 211 and 145, which are ascribed to the cleavage of –SH, C_2H_5 and triazole moiety, respectively, are well observed in the mass spectrum. Schiff bases **I**, **II** and **IV** showed molecular ion peaks at m/z 245, 259 and 287, respectively, with all other fragmentation peaks.

The FAB-mass spectrum of all the complexes exhibited molecular ion peak equivalent of their molecular weight along with other fragmentation peaks. Hence only the representative $Co(C_{12}H_{10}N_5OS)_2$, $Ni(C_{12}H_{10}N_5OS)_2$ and $Cu(C_{12}H_{10}N_5OS)_2$ are discussed here. The spectrum of $Co(C_{12}H_{10}N_5OS)_2$ showed a molecular ion peak M^+ at m/z 603 that is the equivalent of its molecular weight. The fragmentation peaks observed at 476, 331, 204 and 59 correspond to $C_4N_3H_5S$, $C_8N_2H_5O$, $C_4N_3H_5S$ and $C_8N_2H_5O$, respectively. In case of $Ni(C_{12}H_{10}N_5OS)_2$ complex, the molecular ion peak M^+ at m/z 602 corresponds to its molecular weight. The complex exhibited fragmentation peaks at 475, 330, 203 and 58 correspond to cleavages of $C_4N_3H_5S$, $C_8N_2H_5O$, $C_4N_3H_5S$ and $C_8N_2H_5O$, respectively. The spectrum of $Cu(C_{12}H_{10}N_5OS)_2$ complex exhibited a molecular ion peak M^+, equivalent of its molecular weight, at m/z 607 with all other fragmentation peaks.

3.6. *ESR spectrum of $Cu(C_{12}H_{10}N_5OS)_2$ complex*

The ESR spectrum of one representative $Cu(C_{12}H_{10}N_5OS)_2$ has been studied under liquid nitrogen temperature using TCNE as a g marker. ESR spectrum of Cu(II) complex showed g value 2.00277. The $g_\parallel$ and $g_\perp$ values were found to be 2.0156 and 2.1826, respectively. The g_{av} was calculated to be 2.0602. The Cu(II) complex shows reversed axial (compressed octahedral) with $g_\parallel < g_\perp$.

3.7. *Thermal studies of metal complexes*

The thermal behavior of Co(II), Ni(II) and Cu(II) complexes has been studied as a function of temperature, and it is almost the same. Hence, only the representative $Co(C_{12}H_{10}N_5OS)_2$, $Ni(C_{12}H_{10}N_5OS)_2$ and $Cu(C_{12}H_{10}N_5OS)_2$ complexes have been discussed here.

The differential thermo-gravimetry (DTG) curve of the $Co(C_{12}H_{10}N_5OS)_2$ complex showed that the two triazole and two isatin moieties were lost in the regions of 215–245, 310–345, 350–395 and 420–475 °C corresponding to the mass losses of 23.16% (calc. 23.55%), 20.84 (calc. 21.06%), 21.44% (calc. 21.72%) and 23.92% (calc. 24.04%). Finally, the formation of metal oxide took place above 500 °C. The complex $Ni(C_{12}H_{10}N_5OS)_2$ loses all its triazole and isatin moieties in the regions 240–265, 330–340, 350–385 and 430–475 °C, with the mass losses of 21.01% (calc. 21.09%), 23.16% (calc. 23.42%), 23.82% (calc. 24.08%) and 21.39% (calc. 21.76%). The formation of metal oxide took place at 520 °C. In case of $Cu(C_{12}H_{10}N_5OS)_2$ complex, the losses of triazole and isatin moieties were found to be in the region 220–240, 315–345, 355–375 and 440–460 °C corresponding to the mass losses of 23.11% (calc. 23.23%), 20.27% (calc. 20.92%), 21.46% (calc. 21.58%) and 23.47% (calc. 23.88%). Finally, the metal oxide formed at 515 °C.

3.8. *Electrochemistry*

The electrochemical properties of metal complexes, particularly those with sulfur donor atoms, have been studied in order to monitor spectral and structural changes accompanying electron transfer (*38*).

All the Cu(II) complexes showed similar electrochemical behavior. Cyclic voltammogram (Figure 2) of one representative $Cu(C_{12}H_{10}N_5OS)_2$ complex is discussed here. The oxidation peak in the 0.6–0.7 V region and the associated reduction peak in the 0.150–0.250 V region at a scan rate of $0.1\,V\,s^{-1}$ is assigned to the Cu(II)/Cu(III) redox couple. In the cathodic region, an irreversible peak at −1.0059 V and a quasireversible peak at −1.7641 V are observed corresponding to Cu(II)/Cu(I) and Cu(I)/Cu(0) (*39*, *40*). During the reverse scan, the oxidation of Cu(I)/Cu(II) skips over and passes to the Cu(III) state. This was confirmed by the ratio of anodic to cathodic current value of the Cu(II)/Cu(III) couple ($I_{pa}/I_{pc} = 2$).

All the Co(II) and Ni(II) complexes exhibited two quasireversible peaks. The representative current value of the $Co(C_{12}H_{10}N_5OS)_2$ complex is given in Figure 3. A cyclic voltammogram of Co(II) displays two reduction peaks, the first at $E_{pc} = -1.0078\,V$ with an associated oxidation peak at $E_{pa} = -0.2123\,V$ and second reduction peak at $E_{pc} = -1.7897\,V$ with an associated oxidation peak at $E_{pa} = -0.7038\,V$ corresponding to the Co(II)/Co(I) and Co(I)/Co(0), respectively. The value of ΔE_p is 0.7955 and 1.0859 at a scan rate of $0.1\,V\,s^{-1}$ for the first and second redox couples, respectively. This value increases from $\Delta E_p = 0.7542\,V$ at $0.05\,V\,s^{-1}$ to $\Delta E_p = 0.7955$ at $0.1\,V\,s^{-1}$ indicating a kinetic inhibition of the electron transfer process (*41*). The cyclic voltammograms with varied scan rates 0.025, 0.5 and $0.1\,V\,s^{-1}$ (Figure 4) give the further evidence for the quasireversible nature of the Co(II) (3) complex.

A current value of $Ni(C_{12}H_{10}N_5OS)_2$ (7) (Figure 5) shows two reduction peaks corresponding to the Ni(II)/Ni(I) and Ni(I)/Ni(0), first one at $E_{pc} = -0.9874\,V$ with an associated oxidation peak at $E_{pa} = -0.1646\,V$ and second reduction peak at $E_{pc} = -1.6363\,V$ with an associated oxidation peak at $E_{pa} = -0.7080\,V$, respectively. The value of ΔE_p is 0.8228 and 0.9283 at a scan rate of $0.1\,V\,s^{-1}$ for first and second redox couples, respectively, gives the evidence for quasireversible nature of Ni(II) complex.

3.9. In vitro *antimicrobial assay*

The antimicrobial results are systematized in Tables 6 and 7. From the antibacterial studies, it is inferred that the Schiff bases **(I–IV)** were found to be potentially active against *S. aureus* and *B. subtitlis*, and moderately active against *P. auregenosa*. All the Co(II) **(1–4)** and Cu(II) **(9–12)**

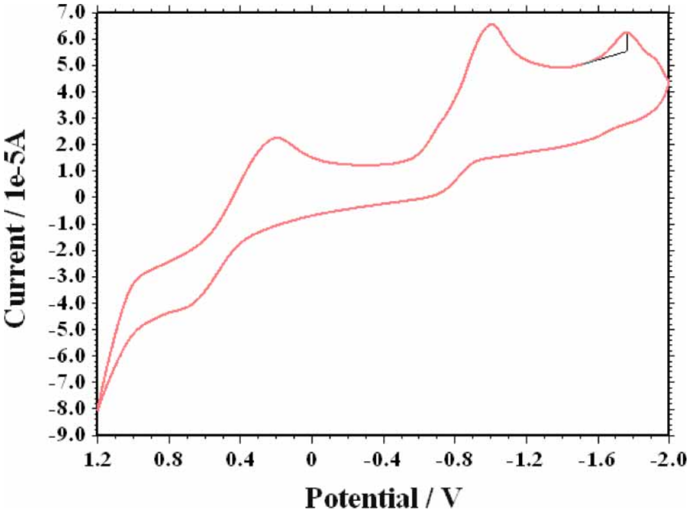

Figure 2. Cyclic voltammogram of $Cu(C_{12}H_{10}N_5OS)_2$ complex (11).

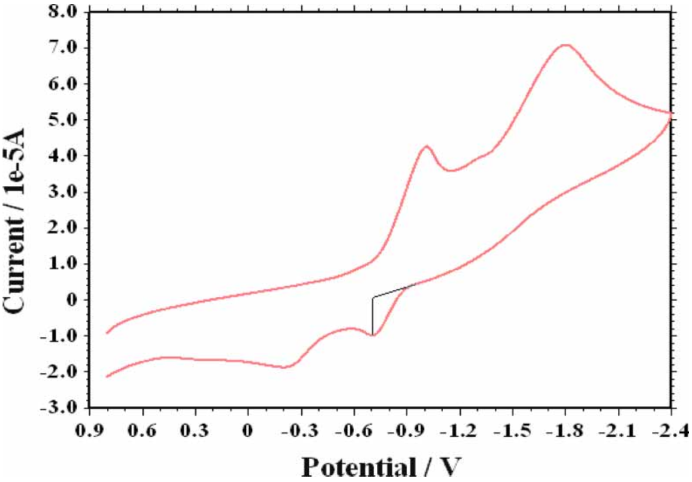

Figure 3. Cyclic voltammogram of Co($C_{12}H_{10}N_5OS)_2$ complex (3) at a scan rate 0.1 V s^{-1}.

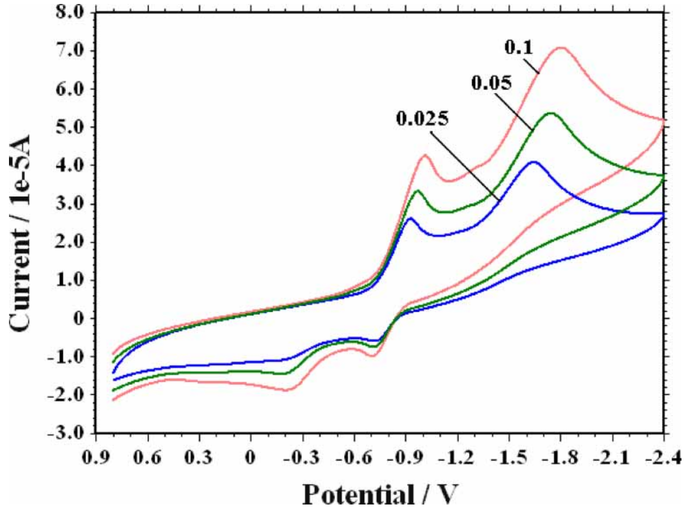

Figure 4. Cyclic voltammogram of Co($C_{12}H_{10}N_5OS)_2$ complex (3) at a scan rate 0.1, 0.05 and 0.025 V s^{-1}.

complexes showed high antibacterial activity against *S. aureus* and *B. subtilis*. In particular, complexes **2, 3, 4, 9, 10, 11** and **12** showed higher activity than the respective Schiff bases. This higher activity of the metal complexes compared with Schiff bases may be due to the change in structure due to coordination, which makes the metal complexes act as more powerful and potent bactereostatic agents, thus inhibiting the growth of the microorganisms (*42–44*). It is suspected that factors such as solubility, conductivity, dipole moment and cell permeability mechanism (influenced by the presence of metal ions) may be the possible reasons for the increase in activity (*45*, *46*).

In case of antifungal activity, the Schiff bases and their Co(II), Ni(II) and Cu(II) complexes were found to be inactive or moderately active. Thus, the data revealed that the newly synthesized compounds possess higher-antibacterial activity than the antifungal nature.

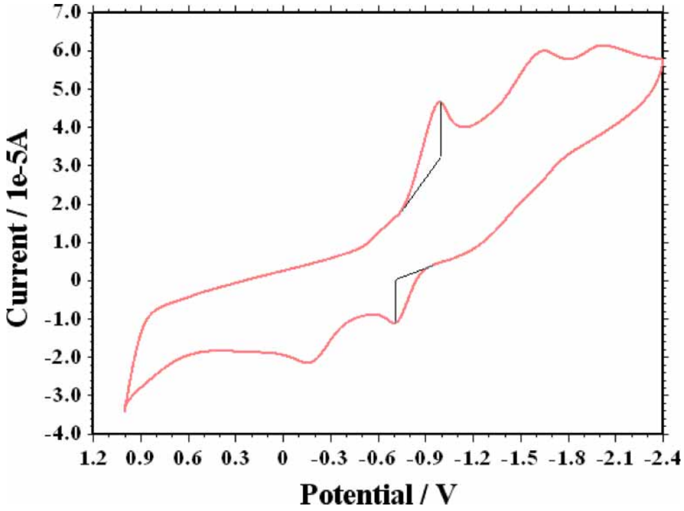

Figure 5. Cyclic voltammogram of Ni($C_{12}H_{10}N_5OS$)$_2$complex (7) at a scan rate of 0.1.

Table 6. Antimicrobial results of Schiff bases.

Compound	Concentration (μg ml^{-1})	Growth inhibition against bacteria in mm				Growth inhibition against fungi in mm	
		S. aureus	*B. subtilis*	*P. auregenosa*	*E. coli*	*A. niger*	*P. crysogenum*
$C_{10}H_7N_5OS$	100	11	8	11	6	10	7
	200	15	12	13	7	12	8
	500	22	21	17	8	13	10
$C_{11}H_9N_5OS$	100	12	7	11	7	11	8
	200	13	14	14	7	11	8
	500	22	20	16	9	13	10
$C_{12}H_{11}N_5OS$	100	12	10	12	7	7	7
	200	13	12	13	7	7	8
	500	20	18	20	9	10	8
$C_{13}H_{13}N_5OS$	100	13	9	11	6	7	7
	200	15	11	14	9	9	9
	500	21	18	20	10	10	9
Streptomycin	500	28	29	35	25	–	–
Nyastatin	500	–	–	–	–	26	25

Note: Less than 12 mm – inactive; 12–16 mm – moderately active; above 16 mm – highly active.

The MIC of some selected compounds, which showed significant activity against selected bacterial and fungi species, were determined. The MIC results of these compounds are presented in Table 8. The results indicated that these compounds were the most active in inhibiting the growth of the tested organisms at a 10 μg ml^{-1} concentration.

4. Conclusion

In this study, the Co(II), Ni(II) and Cu(II) complexes with isatin–triazole Schiff bases were synthesized and characterized. On the basis of different techniques, it is proposed that all the

Table 7. Antimicrobial results of metal complexes.

		Growth inhibition against bacteria in mm				Growth inhibition against fungi in mm	
Compound	Conc. (μg ml^{-1})	*S. aureus*	*B. subtilis*	*P. auregenosa*	*E. coli*	*A. niger*	*P. crysogenum*
$Co(C_{10}H_6N_5OS)_2$	100	7	8	8	7	9	7
	200	16	13	15	8	9	8
	500	22	20	21	10	13	8
$Co(C_{11}H_8N_5OS)_2$	100	8	7	9	8	8	8
	200	14	15	16	8	10	8
	500	24	22	19	12	14	8
$Co(C_{12}H_{10}N_5OS)_2$	100	11	7	8	6	8	8
	200	18	14	14	7	10	8
	500	23	21	19	9	13	13
$Co(C_{13}H_{12}N_5OS)_2$	100	12	8	9	7	7	7
	200	18	14	16	7	10	9
	500	24	23	21	10	14	11
$Ni(C_{10}H_6N_5OS)_2$	100	7	7	8	7	7	8
	200	7	10	8	7	7	8
	500	7	13	10	8	12	10
$Ni(C_{11}H_8N_5OS)_2$	100	7	8	8	8	7	7
	200	8	10	8	8	8	8
	500	8	12	12	8	8	10
$Ni(C_{12}H_{10}N_5OS)_2$	100	9	7	8	7	7	8
	200	11	7	8	7	10	8
	500	14	7	8	9	13	10
$Ni(C_{13}H_{12}N_5OS)_2$	100	10	7	8	8	7	8
	200	12	9	9	9	9	8
	500	13	9	9	10	11	11
$Cu(C_{10}H_6N_5OS)_2$	100	7	8	7	7	6	8
	200	12	14	12	7	8	8
	500	22	24	17	7	12	8
$Cu(C_{11}H_8N_5OS)_2$	100	8	8	8	8	7	7
	200	14	18	16	10	9	8
	500	26	24	22	10	10	8
$Cu(C_{12}H_{10}N_5OS)_2$	100	7	8	7	7	7	9
	200	15	12	16	7	10	9
	500	21	23	24	10	13	12
$Cu(C_{13}H_{12}N_5OS)_2$	100	8	8	7	8	7	9
	200	14	15	16	9	9	11
	500	23	22	21	12	11	12
Streptomycin	500	28	29	35	25	–	–
Nyastatin	500	–	–	–	–	26	25

Note: Less than 12 mm – inactive; 12–16 mm – moderately active; above 16 mm – highly active.

complexes possess octahedral geometry (Figure 6) and the Schiff bases act as versatile tridentate ligands coordinated to metal ion through carbonyl oxygen, nitrogen and sulfur atoms.

The electrochemical properties of the metal complexes investigated in DMF showed most significant two-electron transfer processes. From the *in vitro* antibacterial and antifungal activity against representative bacterial and fungal strains, it is evident that the Schiff bases and their Co(II) and Cu(II) complexes were found to possess high antibacterial activity.

Table 8. Results of minimum inhibitory concentration (µg/ml).

Compound	*S. aureus*	*B. subtilis*	*P. auregenosa*	*E. coli*	*A. niger*	*P. crysogenum*
$C_{10}H_7N_5OS$	10	10	–	–	–	25
$C_{11}H_9N_5OS$	10	10	–	–	25	25
$C_{12}H_{11}N_5OS$	10	25	10	–	–	–
$C_{13}H_{13}N_5OS$	10	25	25	>100	25	–
$Co(C_{10}H_6N_5OS)_2$	25	10	15	25	25	–
$Co(C_{11}H_8N_5OS)_2$	25	10	25	10	10	–
$Co(C_{12}H_{10}N_5OS)_2$	10	10	10	–	>100	25
$Co(C_{13}H_{12}N_5OS)_2$	10	10	10	>100	10	>100
$Ni(C_{10}H_6N_5OS)_2$	–	25	–	>100	25	25
$Ni(C_{11}H_8N_5OS)_2$	–	>100	>100	>100	>100	25
$Ni(C_{12}H_{10}N_5OS)_2$	10	–	–	>100	10	>100
$Ni(C_{13}H_{12}N_5OS)_2$	>100	–	–	>100	–	–
$Cu(C_{10}H_6N_5OS)_2$	10	10	>100	>100	25	–
$Cu(C_{11}H_8N_5OS)_2$	10	>100	10	25	>100	–
$Cu(C_{12}H_{10}N_5OS)_2$	10	10	10	25	10	25
$Cu(C_{13}H_{12}N_5OS)_2$	10	10	15	10	>100	25

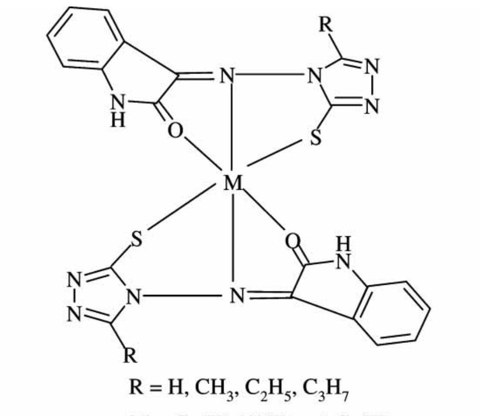

R = H, CH_3, C_2H_5, C_3H_7

M = Co(II), Ni(II) and Cu(II)

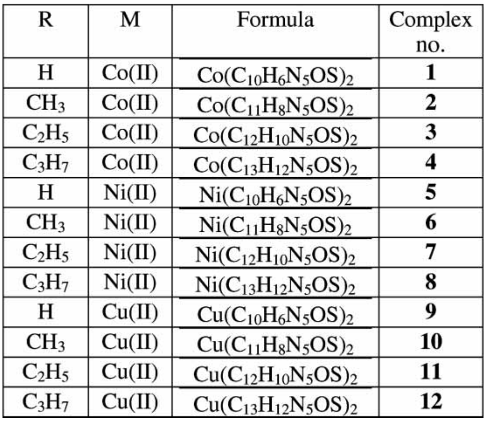

R	M	Formula	Complex no.
H	Co(II)	$Co(C_{10}H_6N_5OS)_2$	**1**
CH_3	Co(II)	$Co(C_{11}H_8N_5OS)_2$	**2**
C_2H_5	Co(II)	$Co(C_{12}H_{10}N_5OS)_2$	**3**
C_3H_7	Co(II)	$Co(C_{13}H_{12}N_5OS)_2$	**4**
H	Ni(II)	$Ni(C_{10}H_6N_5OS)_2$	**5**
CH_3	Ni(II)	$Ni(C_{11}H_8N_5OS)_2$	**6**
C_2H_5	Ni(II)	$Ni(C_{12}H_{10}N_5OS)_2$	**7**
C_3H_7	Ni(II)	$Ni(C_{13}H_{12}N_5OS)_2$	**8**
H	Cu(II)	$Cu(C_{10}H_6N_5OS)_2$	**9**
CH_3	Cu(II)	$Cu(C_{11}H_8N_5OS)_2$	**10**
C_2H_5	Cu(II)	$Cu(C_{12}H_{10}N_5OS)_2$	**11**
C_3H_7	Cu(II)	$Cu(C_{13}H_{12}N_5OS)_2$	**12**

Figure 6. Structure of metal complexes.

References

(1) Shujuan, S.; Hongxiang, L.; Gao, Y.; Fan, P.; Ba, M.; Ge, W.; Wang, X. *J. Pharm. Biomed. Anal.* **2004,** *34,* 1117–1124.
(2) Werreck, G.; Six, K.; Mootor, G.V.; Baert, L.; Peeters, J.; Brewster, M.E. *Int. J. Pharm.* **2003,** *251,* 165–174.
(3) Panda, S.; Mishra, R.; Panda, A.K.; Satpathy, K.C. *J. Indian Chem. Soc.* **1989,** *66,* 472–474.
(4) Andrzej, O.; Shunzhong, Y.; McGarvey, B.R.; Mislankar, A.; Drake, J.E. *Inorg. Chem.* **1991,** *30,* 3167–3174.
(5) Nieawenhais, H.A.; Haasnoot, J.G.; Hage, R.; Reedijk, J.; Snoeck, T.L.; Stufkens, D.J.; Vos, J.G. *Inorg. Chem.* **1991,** *30,* 48–54.
(6) Cornelissen, J.P.; van Diemen, J.H.; Groeneveld, L.R.; Haasnoot, J.G.; Spek, A.L.; Reedijk, J. *Inorg. Chem.* **1992,** *31,* 198–202.
(7) Varma, R.C.; Varma, K.; Verma, R.K.; Bhattacharjee, N.C. *J. Indian Chem. Soc.* **1992,** *69,* 577–578.
(8) Mishra, L.; Said, M.K. *Indian J. Chem.* **1996,** *35A,* 304–307.
(9) Patil, S.A.; Badiger, B.M.; Kudari, S.M.; Kulkarni, V.H. *Transit. Met. Chem.* **1983,** *8,* 238–240.
(10) Badiger, B.M.; Patil, S.A.; Kudari, S.M.; Kulkarni, V.H. *Rev. Roum. Chim.* **1986,** *31,* 849–855.
(11) Yadawe, M.S.; Patil, S.A. *Transit. Met. Chem.* **1997,** *22,* 220–224.
(12) Avaji, P.G.; Reddy, B.N.; Badami, P.S.; Patil, S.A. *Transit. Met. Chem.* **2006,** *31,* 842–848.
(13) Daisley, R.W.; Shah, V.K.; *J. Pharm. Sci.* **1984,** *73,* 407–408.
(14) Pandeya, S.N.; Sriram, D.; Declecq, E.; Pannecouque, C.; Mitvrouw, M. *Indian J. Pharm. Sci.* **1999,** *60,* 207–212.
(15) Pandeya, S.N.; Dimmock, J.R. *Pharmazie* **1993,** *48,* 659–666.
(16) Cerchiaro, G.; Ferreira, A.M.D. C. *J. Braz. Chem. Soc.* **2006,** *17* (8), 1473–1485.
(17) Pandeya, S.N.; Siram, D.; Nath, G.; Declercq, E. *Eur. J. Pharm. Sci.* **1999,** *9,* 25–31.
(18) Sridhar, S.K.; Pandeya, S.N.; Stables, J.P.; Ramesh, A. *Eur. J. Pharm. Sci.* **2002,** *16,* 129–132.
(19) Silva, J.F.M.; Garden, S.J.; Pinto, A.C. *J. Braz. Chem. Soc.* **2001,** *12,* 273–324.
(20) Hassaan, A.M.A. *Transit. Met. Chem.* **1990,** *15,* 283–285.
(21) Hassaan, A.M.A. *Indian J. Chem.* **1997,** *36,* 241–243.
(22) West, D.X.; El-Sawaf, A.K.; Bain, G.A. *Transit. Met. Chem.* **1998,** *23,* 1–6.
(23) Heng-Shan, D.; Bin, Q.; Kun, W.; Qing-Lian, W.; Zi-Yi, Z. *Magn. Reson. Chem.* **2000,** *38,* 210–212.
(24) Papakonstantinou-Garuofalia, S.S.; Tani, E.; Todoulou, O.; Papadaki-Valiraki, A.; Filippators, E.; Clercq, E.D.; Kourounakis, P.N. *J. Pharm. Pharmacol.* **1998,** *50,* 117–124.
(25) Sadana, A.K.; Mirza, Y.; Aneja, K.R.; Prakash, O. *Eur. J. Med. Chem.* **2003,** *38,* 533–536.
(26) Singh, G.; Singh, P.A.; Singh, K.; Singh, D.P.; Handa, R.N.; Dubey, S.N. *Proc. Nat. Acad. Sci. Ind.* **2002,** *72A,* 87–94.
(27) Neena, S.; Sunita, H.; Jyoti, S.; Vanita, P.; Agarwala, B.V. *Synth. React. Inorg. Met. Org. Chem.* **1992,** *22,* 1283–1293.
(28) Soliman, A.A.; Linert, W. *Thermochim. Acta* **1999,** *333,* 67–75.
(29) Nakamoto K. *Infrared Spectra of Inorganic and Coordination Compounds;* Wiley-Interscience: New York, 1970.
(30) Cerchiaro, G.; Saboya, P.L.; Ferreira, A.M.C.; Tomazela, D.M.; Eberlin, M.N. *Transit. Met. Chem.* **2004,** *29,* 495–504.
(31) Murukan, B.; Bhageerethi, S.K.; Kochukittan, M. *J. Coord. Chem.* **2007,** *60,* 1607–1617.
(32) Singh, K.; Barwa, M.S.; Tyagi, P. *Eur. J. Med. Chem.* **2006,** *41,* 147–153.
(33) Chandra, S.; Kumar, A. *J. Indian. Chem. Soc.* **2007,** *84,* 325–328.
(34) El-Sawaf, A.K.; West, D.X.; El-Saied, F.A.; El-Bahnasawy, R.M. *Transit. Met. Chem.* **1998,** *23,* 649–655.
(35) Liu, H.; Wang, H.; Gao, F.; Niu, D.; Lu. Z. *J. Coord. Chem.* **2007,** *60,* 2671–2678.
(36) Dholakiya, P.P.; Patel, M.N. *Synth. React. Inorg. Met. Org. Nano Met. Chem.* **2002,** *32,* 819–829.
(37) Singh, D.P.; Kumar, R.; Malik, V.; Tyagi, P. *Transit. Met. Chem.* **2007,** *32,* 1051–1055.
(38) Bond, A.M.; Martin, R.L. *Coord. Chem. Rev.* **1984,** *54,* 23–98.
(39) Srinivasan, S.; Athappan, P.; Rajagopal, G. *Transit. Met. Chem.* **2001,** *26,* 588–593.
(40) Olson, D.C.; Vasilevskis, J. *Inorg. Chem.* **1971,** *10,* 463–470.
(41) Bard, A.J.; Faulkner, L.R. *Electrochemical Methods,* 2nd Ed.; John Wiley: New York, 2001.
(42) Kulkarni, A.; Avaji, P.G.; Bagihalli, G.B.; Patil, S.A.; Badami, P.S. *J. Coord. Chem.* **2009**, *62,* 481–492.
(43) Bagihalli, G.B.; Avaji, P.G.; Patil, S.A.; Badami, P.S. *Eur. J. Med. Chem.* **2008**, *43,* 2639–2649.
(44) Chohan, Z.H.; Pervez, H.; Rauf, A.; Khan, K.M.; Supuran, C.T. *J. Enzyme Inhib. Med. Chem.* **2004**, *19,* 417–423.
(45) Chohan, Z.H.; Supuran, C.T.; Scozzafava, A. *J. Enzyme Inhib. Med. Chem.* **2004,** *19* (1), 79–84.
(46) Chohan, Z.H.; Praveen, M. *Appl. Organomet. Chem.* **2001,** *15,* 617–625.